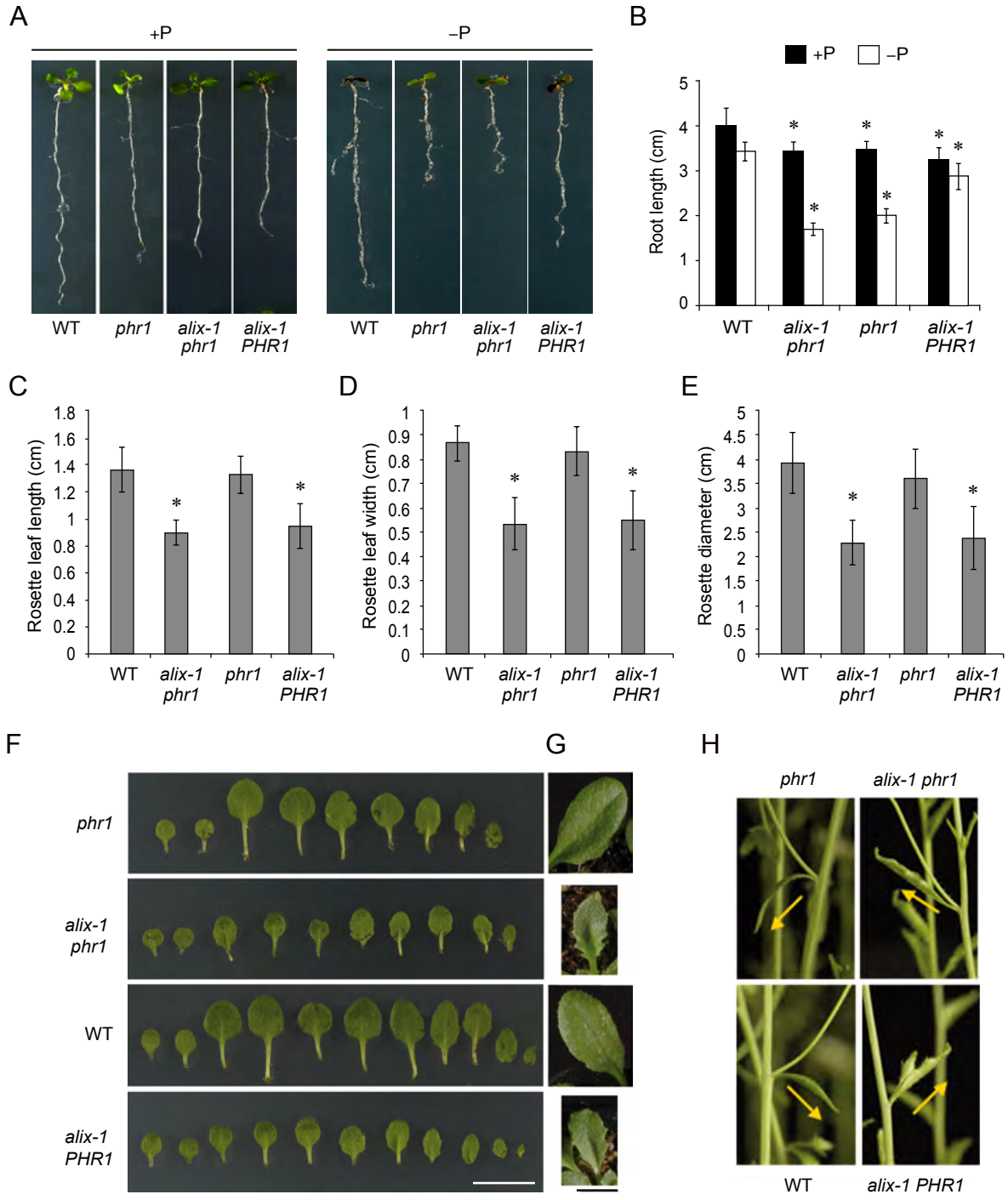

Supplemental Figure 1. Morphological comparisons between *alix-1*, *phr1*, and wild-type (WT) controls.

(A and B) Root length analysis of WT, *phr1*, *alix-1 phr1* and *alix-1 PHR1* plants grown under different Pi supply. Error bars indicate standard deviations.

(C to E) Rosette leaf length and width, and rosette diameter measurements. Same genotypes as in (A) were analyzed. In (B to E) n = 10.

(F) Rosette leaves and petiole phenotypes of plants corresponding to the wild-type, *phr1*, *alix-1 phr1* and *alix-1 PHR1* backgrounds grown in Pi-rich medium for 20 days. Bars = 1 cm.

(G) Details of rosette leaves of plants corresponding to genotypes as above grown in soil for 35 days. Bars = 1 cm.

(H) Pictures showing cauline leaves of plants grown in soil for 49 days. The arrows indicate the direction leaves are pointing.

p<0.01 (Student's t test) with respect to the WT in the same experimental conditions.

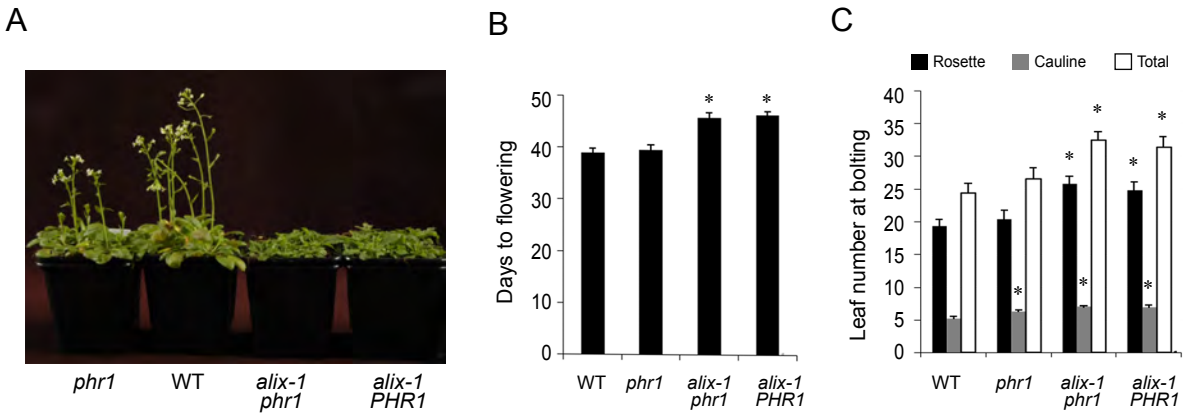

Supplemental Figure 2. Flowering time defects in *alix-1* mutants.
(A) Phenotype of 40-day-old plants corresponding to the wild-type (WT), *phr1*, *alix-1 phr1* and *alix-1 PHR1* backgrounds grown in soil under long day conditions.
(B and C) Histograms showing flowering-time measurements for genotypes described above grown under long day conditions. Flowering time was measured as the number of days to flowering (B) or leaves at bolting (C). The error bars represent standard deviations from sample sizes of at least 25 plants. Statistically significant differences with respect to wild-type plants ($p < 0.05$, according to Student's t test) are marked with asterisks.

A

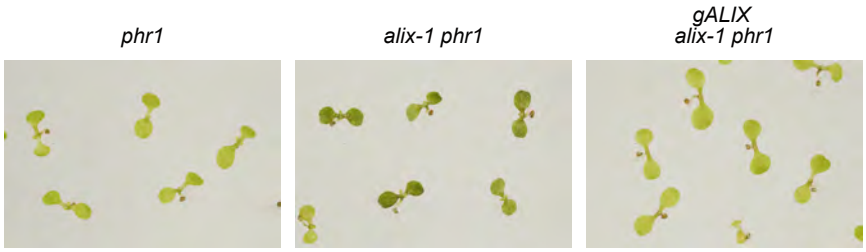

B

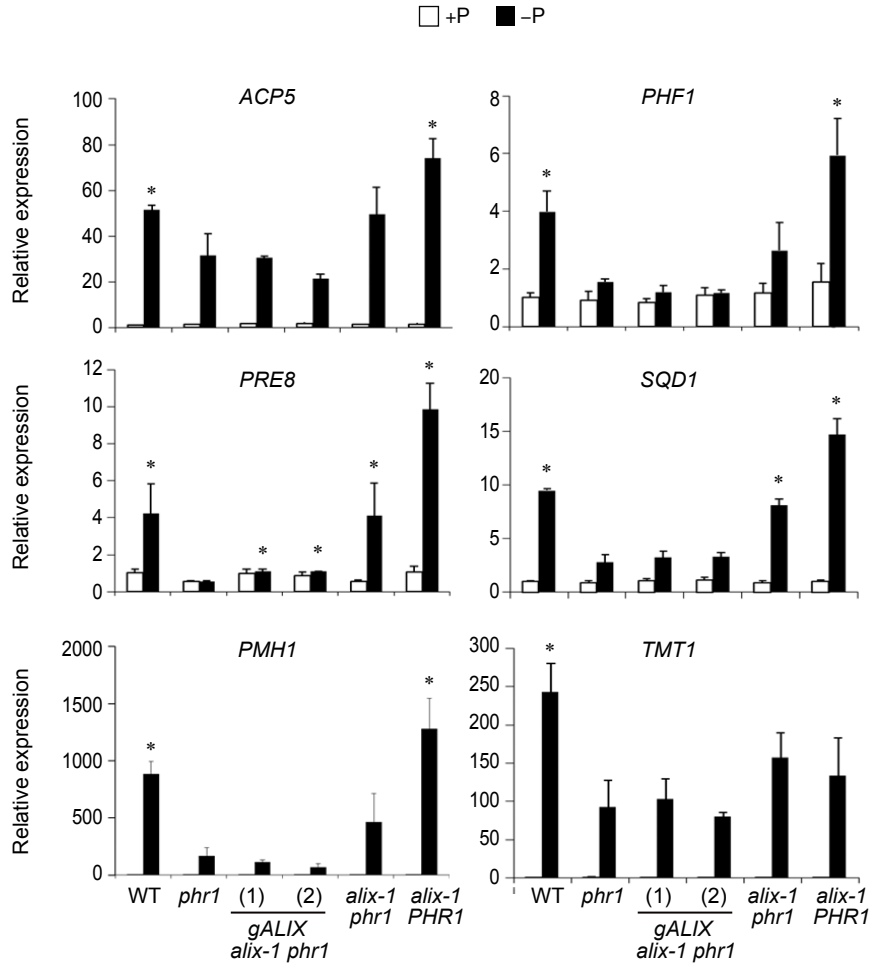

Supplemental Figure 3. Complementation of *alix-1* mutant defects.
(A) Plants corresponding to *phr1*, *alix-1 phr1* and *alix-1 phr1* transformed with a construct containing the *ALIX* genomic region (*gALIX alix-1 phr1*) were grown in Pi-deficient medium for 12 days.
(B) RT-qPCR analysis of Pi-starvation induced gene expression in 10-day-old plants grown under low Pi (-P; 30 μM Pi) and Pi-rich (+P; 500 μM Pi) conditions. Plants corresponded to wild-type (WT), *phr1*, two independent *alix-1 phr1* lines transformed with a construct containing the *ALIX* genomic region (*gALIX alix-1 phr1*), *alix-1 phr1,* and *alix-1 PHR1*. *ACTIN8* was used as a housekeeping reference gene. Expression levels are relative to Pi-rich grown wild-type values, which were normalized to 1. Data represent the mean of three biological replicates, each consisting of sample material pooled from 15-20 plants from different plates, with standard deviation.
* $p<0.05$ (Student's t test) with respect to the *phr1* mutant in the same experimental conditions.

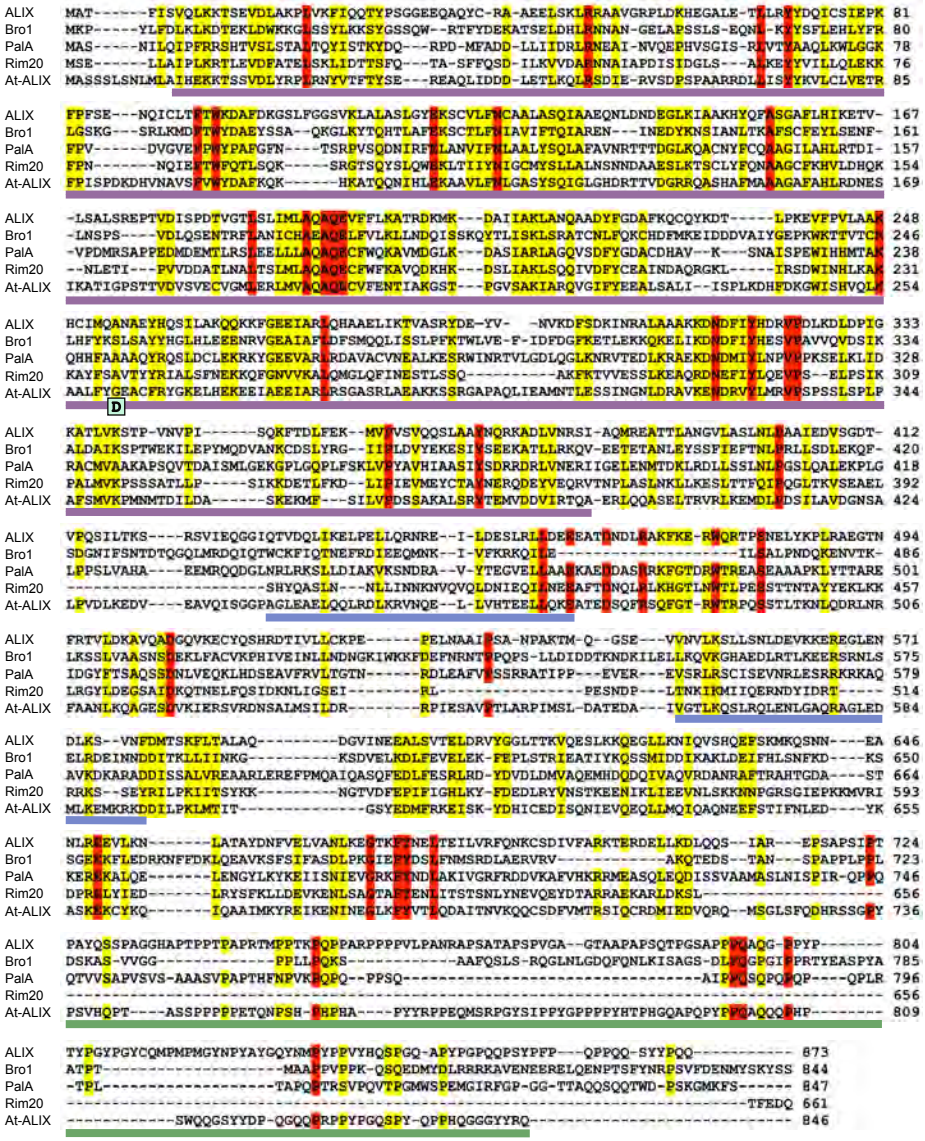

Supplemental Figure 4. Multiple sequence alignment of ALIX-related proteins. Protein sequences include At-ALIX and homolog proteins in mammals (ALIX), *Aspergillus* (PalA) and yeast (Bro1 and Rim20). The alignment was obtained using the T-COFFEE program (Notredame et al., 2000). Amino acids in red correspond to residues conserved in all proteins displayed and in yellow are those that are conserved in most of them. The Bro1, coiled-coil and proline-rich domains as in AtALIX are underlined in purple, blue and green, respectively. The position of the amino acid substitution (Gly260-to-Asp) caused by the *alix-1* mutation is indicated in At-ALIX.

Notredame, C., Higgins, D.G., and Heringa, J. (2000). T-Coffee: A novel method for fast and accurate multiple sequence alignment. J Mol Biol 302, 205-217.

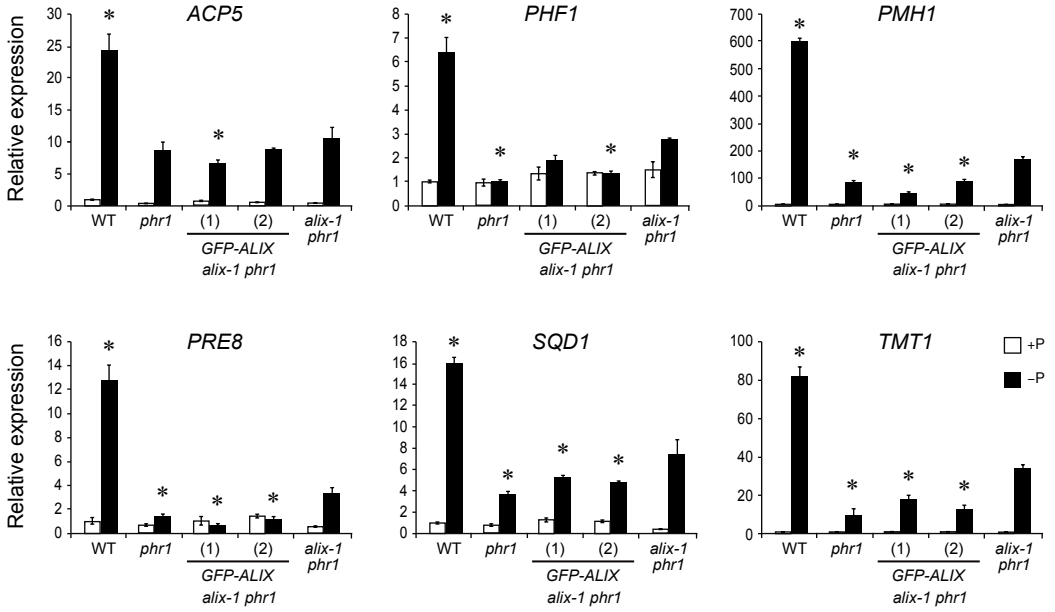

Supplemental Figure 5. Complementation of transcriptional defects in *alix-1* mutants using a protein fusion of ALIX to GFP.

RT-qPCR analysis of the expression of representative *Pi-STARVATION INDUCED* (*PSI*) genes in WT, *phr1*, *alix-1 phr1* and *ALIXpro:GFP-gALIX* (two independent transgenic lines) seedlings grown under low Pi (-P; 30 μM Pi) and Pi-rich (+P; 500 μM Pi) conditions. *ACTIN8* was used as a housekeeping reference gene. Expression levels are relative to Pi-rich grown wild-type values, which were normalized to 1. Data represent the mean of three biological replicates, each consisting of sample material pooled from 15-20 plants from different plates, with standard deviation.

**p<0.05* (Student's t test) with respect to the *alix-1 phr1* in the same experimental conditions.

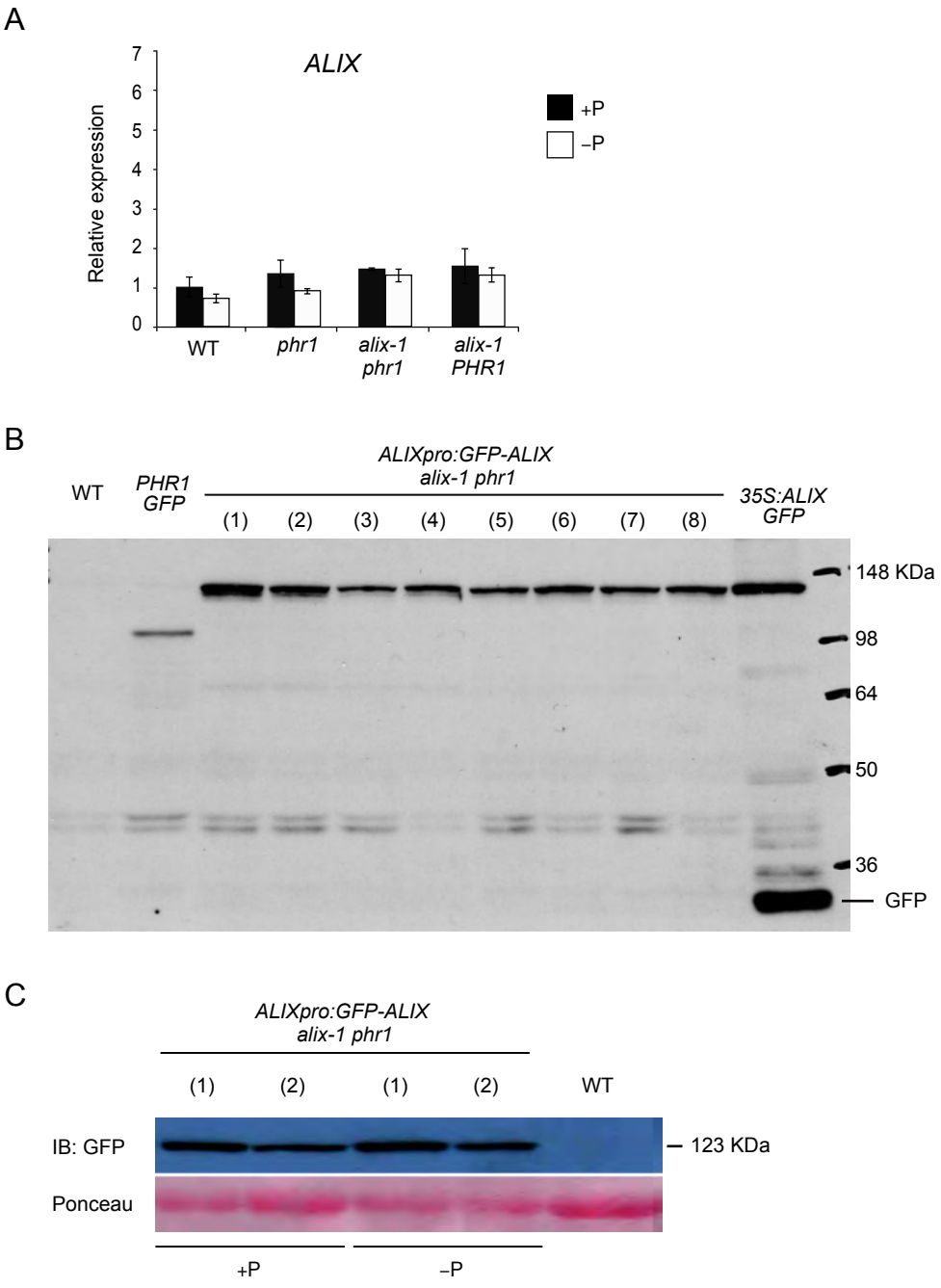

Supplemental Figure 6. *ALIX* gene expression and GFP-ALIX protein accumulation under different Pi supply conditions.

(A) RT-qPCR analysis of *ALIX* gene expression in 10-day-old wild-type (WT), *phr1*, *alix-1 phr1*, and *alix-1 PHR1* plants grown under low Pi (-P; 30 μM Pi) and Pi-rich (+P; 500 μM Pi) conditions. *ACTIN8* was used as a housekeeping reference gene. Expression levels are relative to Pi-rich grown wild-type values, which were normalized to 1. Data represent the mean of three biological replicates with standard deviation.

(B) Immunoblots of protein extracts from 8 independent *alix-1 phr1* lines harboring the *ALIX* genomic region fused to *GFP* under the control of the *ALIX* promoter (*ALIXpro:GFP-gALIX*) compared to that of an ALIX-GFP overexpressing line (*35S:ALIX-GFP*) . PHR1-GFP extracts were used as a control.

(C) Immunoblots of protein extracts from two independent *ALIXpro:GFP-gALIX* lines grown in Pi-deficient (-P) and Pi-rich (+P) media for 10 days.

Anti-GFP antibody was used to detect the GFP fusions. Ponceau staining was used as loading control.

A

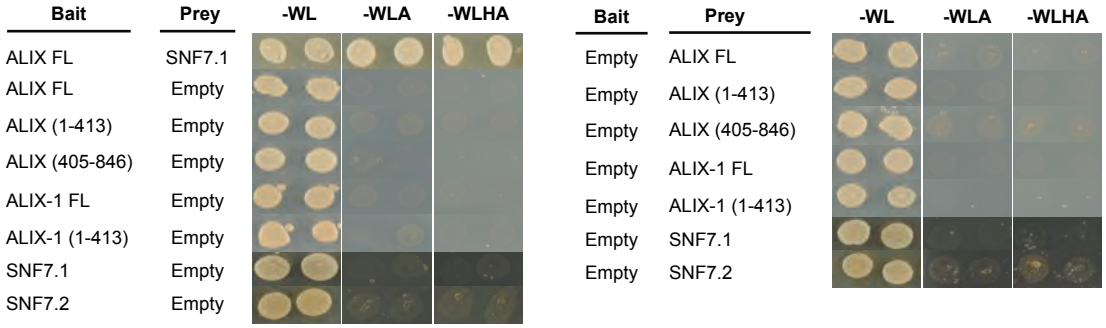

B

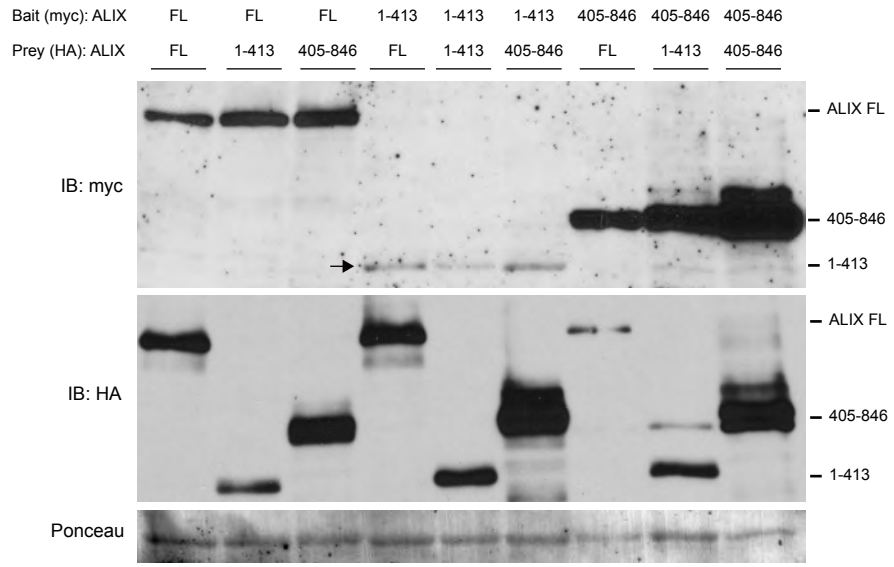

C

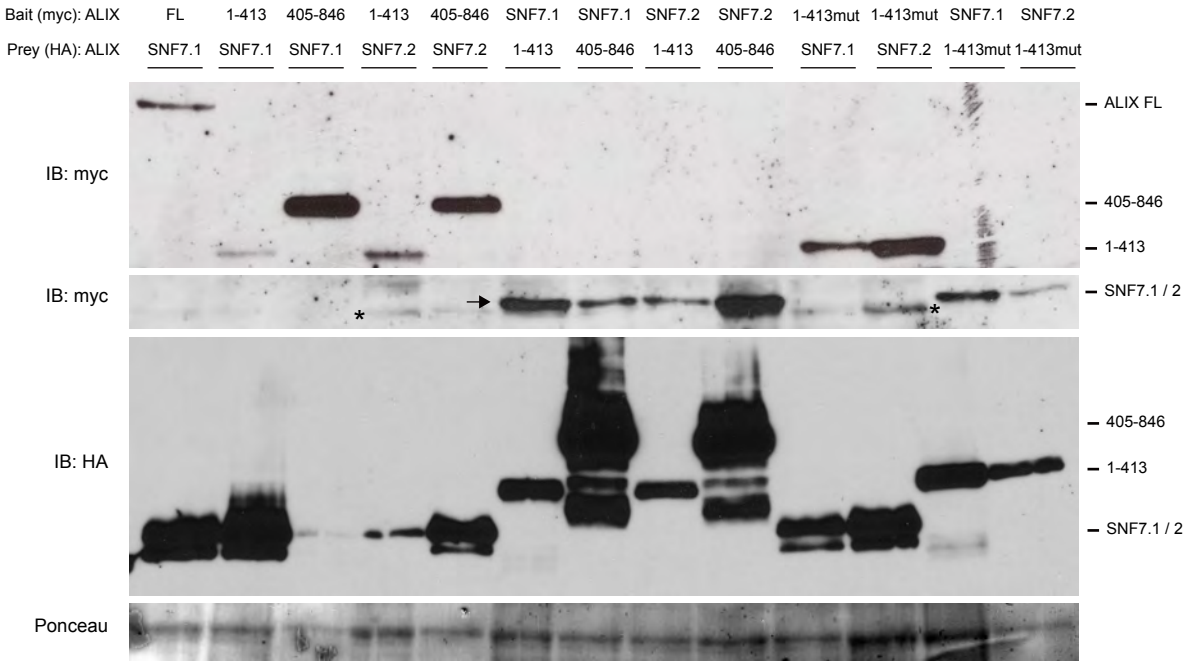

Supplemental Figure 7. Negative controls and expression analysis of bait and prey fusions used in yeast-two hybrid assays displayed in Figures 3 and 5.

(A) Negative controls for yeast-two hybrid assays in which full-length (FL) and truncated versions (comprising the Bro1 domain, aa 1-413; or the coiled coils plus the Pro-rich region, aa 405-846) of ALIX, constructs containing the *alix-1* mutation (ALIX-1; right panels), and SNF7 proteins were cotransformed with the corresponding empty vectors.Transformed yeast cells were grown in SD-WL medium as a transformation control and in SD-WLA and SD-WLHA media for interaction assays.

(B and C) Total protein extracts from yeast clones expressing bait and prey fusions as indicated were immunoblotted using anti-myc (detects Baits) and anti-HA (detects Preys) antibodies. Ponceau staining of membranes was used as loading control. Arrows point to proteins bands corresponding to ALIX 1-413 (in B) or SNF7 fusions (in C). Asterisks indicate non-specific bands close to SNF7 protein bands.

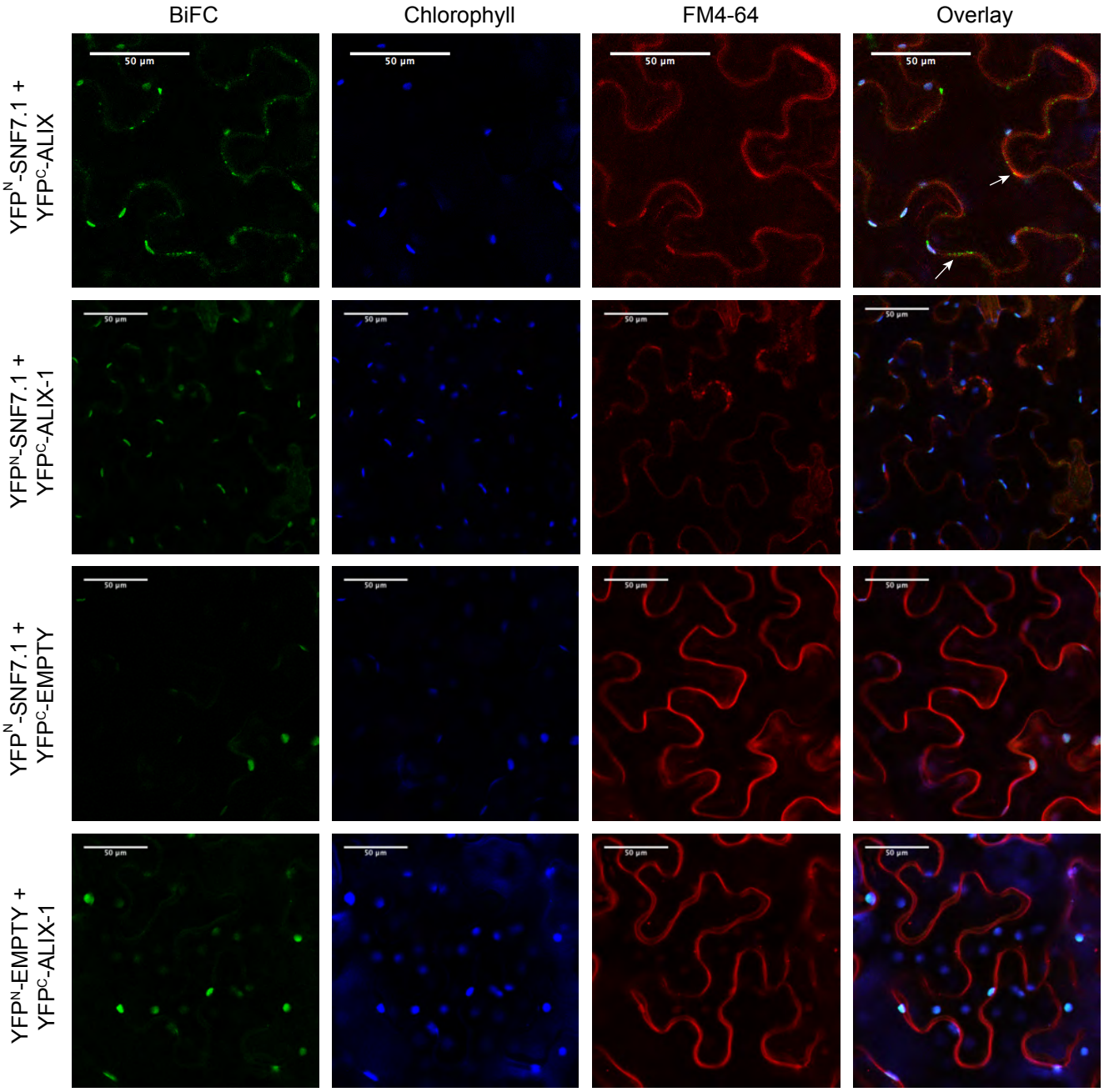

Supplemental Figure 8. BiFC assays showing interaction between ALIX and SNF7.1 in vivo.

Bimolecular Fluorescence Complementation (BiFC) assays show that ALIX, but not a version containing the *alix-1* mutation, interacts with SNF7.1 in vivo. 5 µM FM-4-64 was injected in *N. benthamiana* leaf epidermal cells expressing different construct combinations as indicated. Leaves were observed by confocal imaging after 60 min. Reconstitution of YFP fluorescence indicates that the corresponding ALIX and SNF7 constructs directly interact. White arrows show YFP fluorescence colocalization with FM4-64 signal (red channel). Plastid autofluorescence due to chlorophyll is shown in the blue channel. Bars = 50 µm.

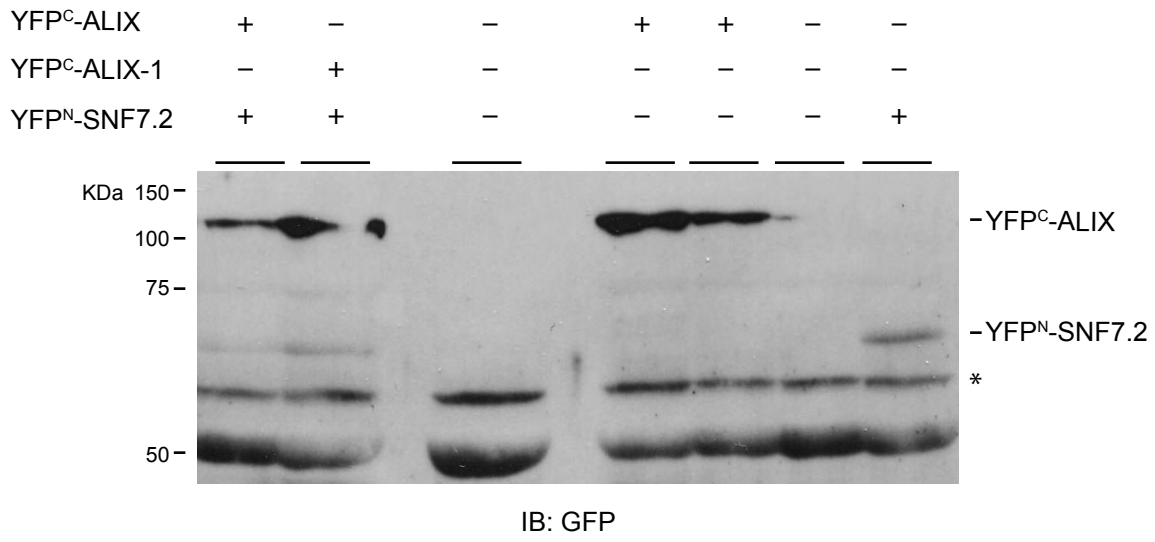

Supplemental Figure 9. Expression analysis of protein fusions used in BiFC assays displayed in Figure 5.
(A) Protein extracts from *Nicotiana benthamiana* leaves agroinfiltrated with indicated construct combinations were immunoblotted using polyclonal anti-GFP, detecting both YFP-C and YFP-N protein fusions. The position of bands corresponding to wild-type and ALIX-1 mutant versions of ALIX, and that of SNF7.2, fused to YFP fragments are shown. An asterisk indicates the position of a non-specific band used as loading control.

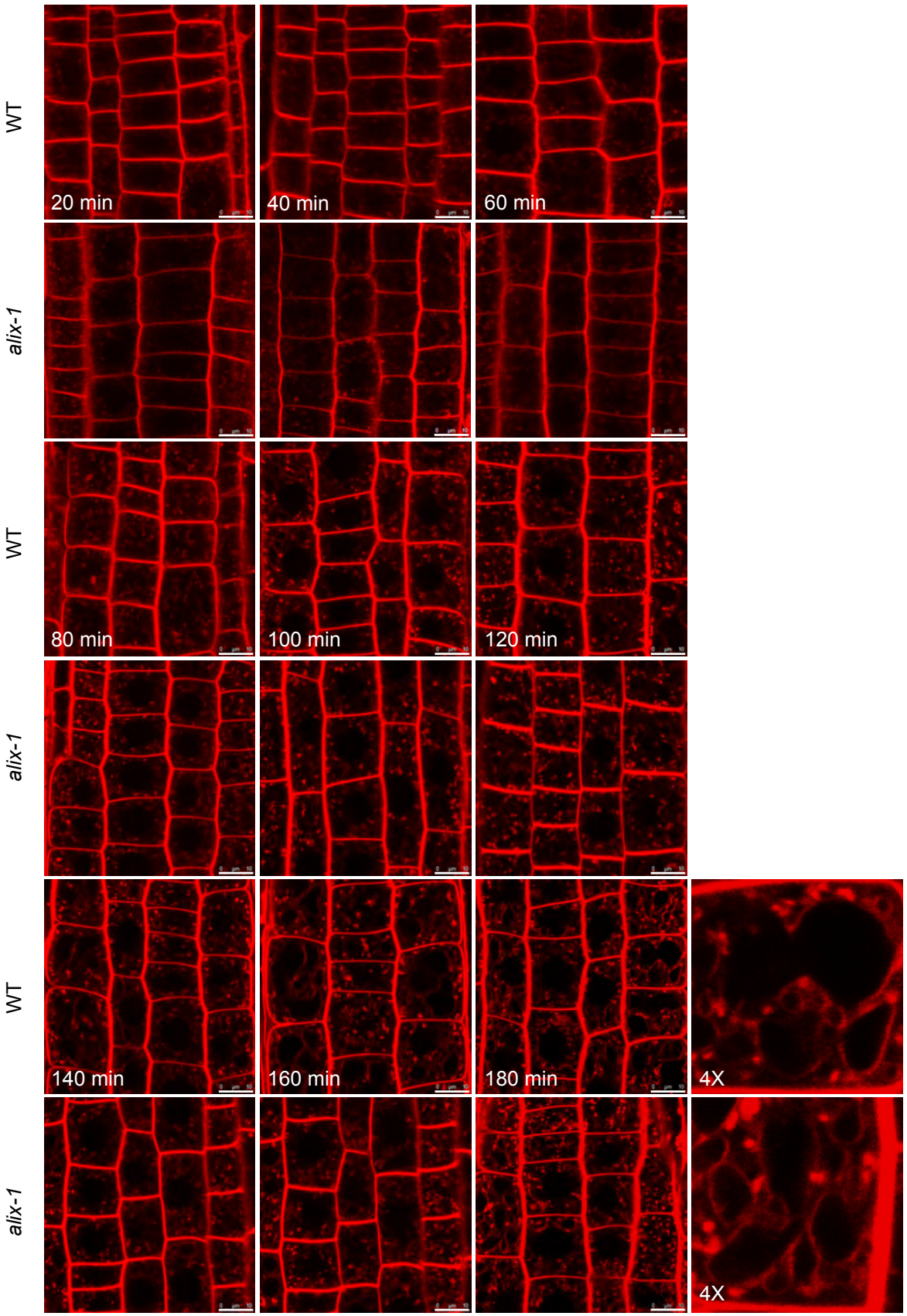

Supplemental Figure 10. Analysis of endocytosis and vesicle trafficking in *alix-1* mutants.
Five-day-old wild-type (WT) and *alix-1* mutant plants were treated with 2 µM FM4-64 for 5 min. After washing, root cells were visualized by confocal imaging every 20 min for 3 h.
4X enlarged images of FM4-64 stained cells after 180 min are shown.

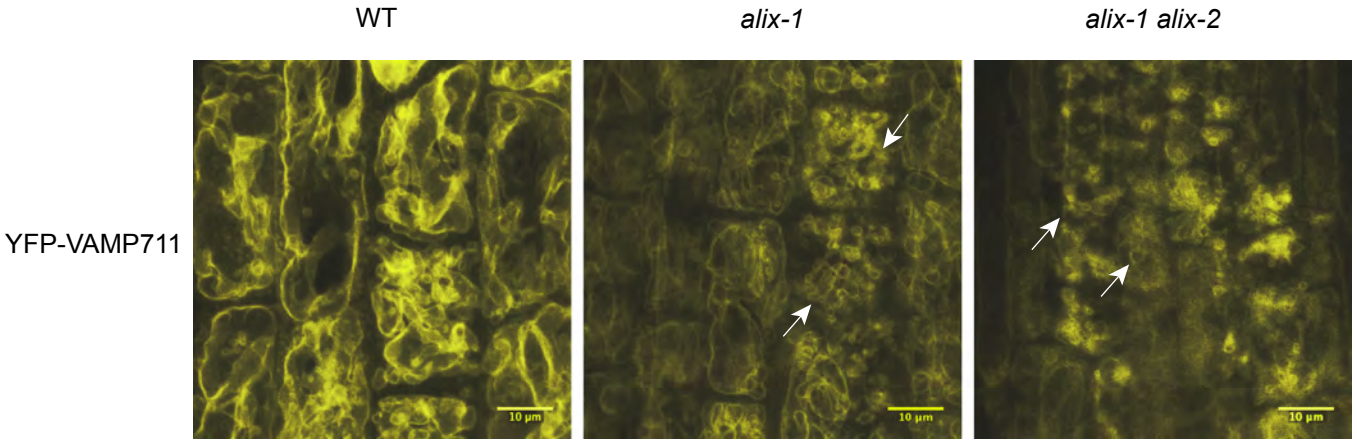

Supplemental Figure 11. Mutants displaying reduced ALIX function are defective in vacuolar size and morphology.
Confocal images of root cells from 5-day-old wild-type (WT), *alix-1* and transheterozygous *alix-1 alix-2* mutants overexpressing the tonoplast marker YFP-VAMP711 (Geldner et al., 2009). Increased number of vacuoles of smaller size (shown by arrows) than those in the WT control can be observed in *alix-1* and *alix-1 alix-2* mutants. Bars = 10 µm.

Geldner, N., Denervaud-Tendon, V., Hyman, D.L., Mayer, U., Stierhof, Y.D., and Chory, J. (2009). Rapid, combinatorial analysis of membrane compartments in intact plants with a multicolor marker set. Plant J. 59, 169-178.

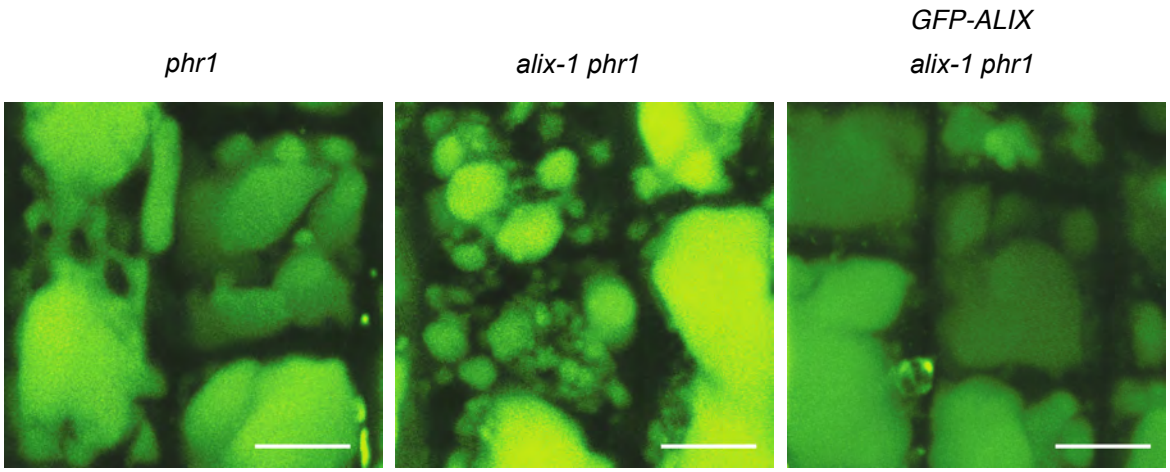

Supplemental Figure 12. Vacuolar morphology defects in *alix-1* mutants can be rescued by expression of a GFP-ALIX fusion.
Vacuole staining with BCECF-AM in root cells from 5-day-old *phr1*, *alix-1* and *alix-1 phr1* mutants harboring the *ALIXpro:GFP-gALIX* construct (*GFP-ALIX*). In contrast to the *alix-1* mutant, *GFP-ALIX alix-1* plants display similar vacuole number and size that the *phr1* parental line. Bars = 10 µm.

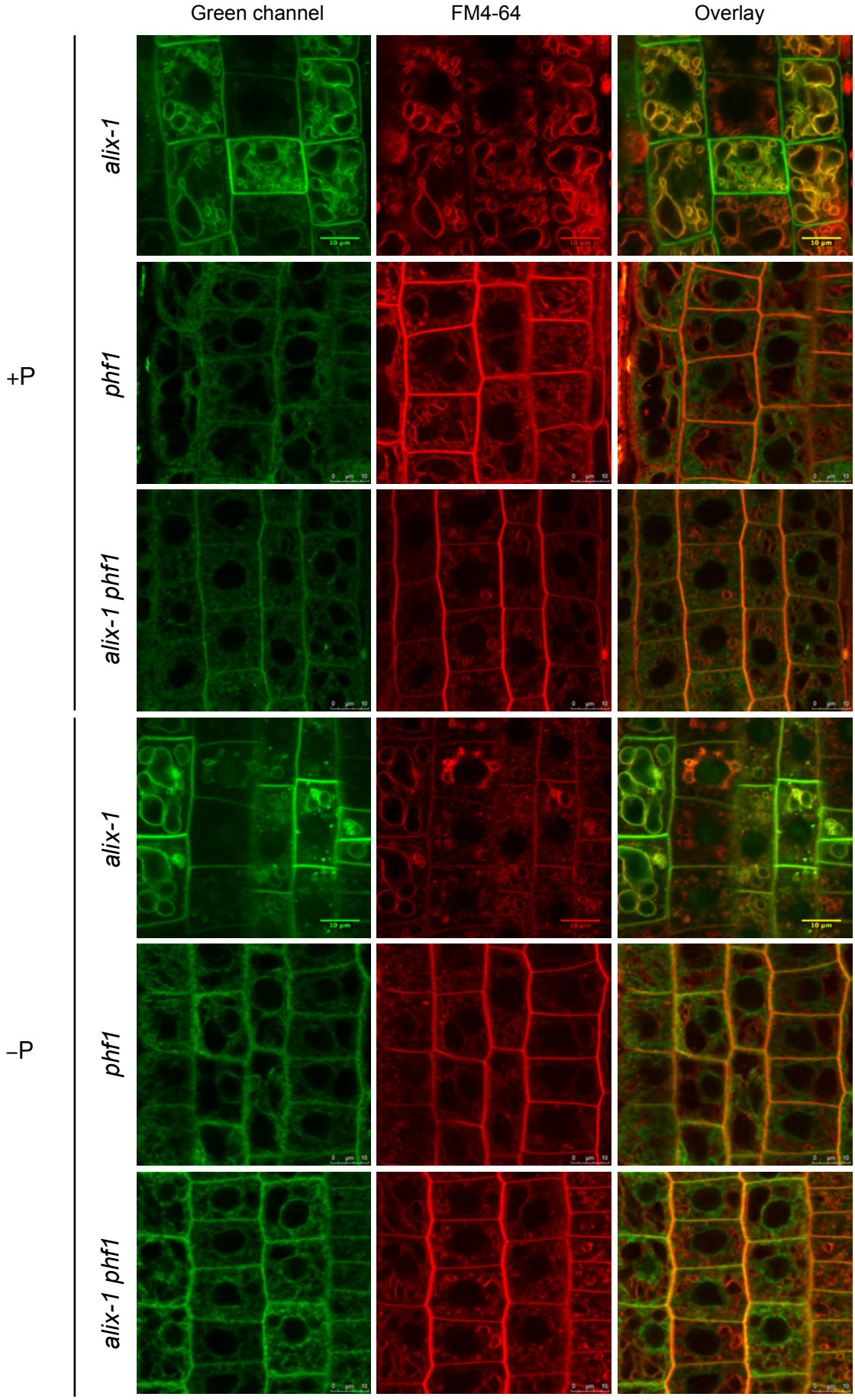

Supplemental Figure 13. ALIX acts as a later stage than PHF1 during PHT1;1 trafficking. Confocal images of root epidermal cells from 5 day-old *35S:PHT1;1-GFP* seedlings in the *alix-1*, *phf1* and *alix-1 phf1* backgrounds grown under Pi-low and -rich conditions. Seedlings were treated with 2µM FM4-64 for 5 min and visualized after 180 min. Bars = 10 µm.

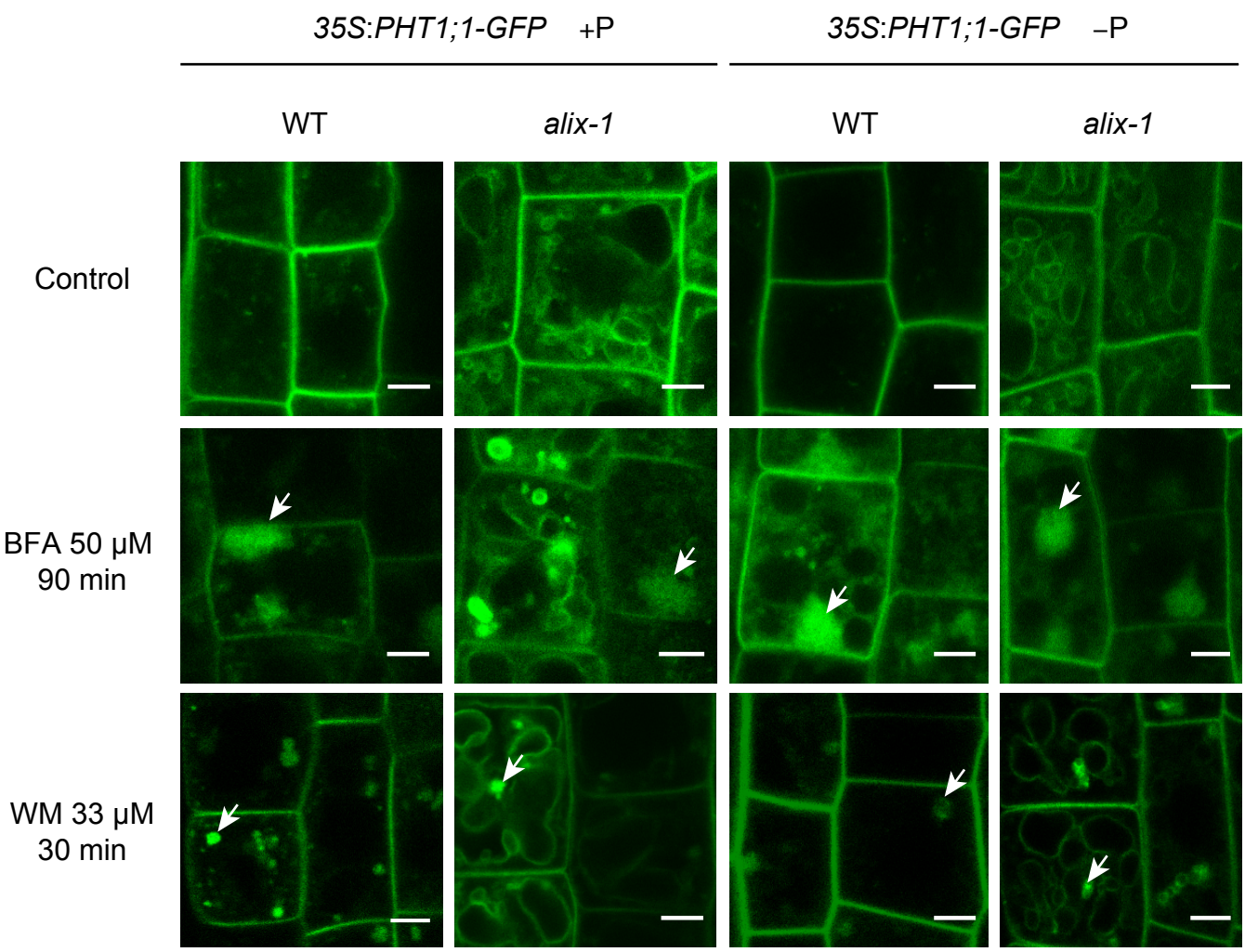

Supplemental Figure 14. *alix-1* mutation does not alter PHT1;1 localization in sorting endosomes and brefeldin bodies.
5-day-old *35S:PHT1;1-GFP* seedlings in wild-type (WT) and *alix-1* backgrounds, grown in Pi-deficient (-P) or Pi-rich conditions (+P), were treated with 50 µM brefeldin A (BFA) for 90 min or with 33 µM wortmannin (WM) for 30 min. Arrows in confocal microscopy images point to brefeldin bodies or WM-enlarged sorting endosomes, according to the treatment, in which PHT1;1-GFP fusions localize. Bars = 10 µm.

Supplemental Table 1. Phenotypic characterization of the progeny obtained from heterozygous *alix-1* plants. Anthocyanin accumulation was analyzed in the F2 progeny (n=500) of a cross between *alix-1 phr1* and *phr1* seedlings grown under low Pi conditions for 10 days.

Observed phenotype frequency (%)		Expected phenotype frequency (%)[a]	
phr1	*alix-1 phr1*	*phr1*	*alix-1 phr1*
85	15	75	25

[a] Expected phenotype frequency for a recessive mutation

Supplemental Table 2. Segregation data from selfed *alix*-2 *ALIX* progeny.

Genotype	Observed	Observed frequency (%)	Expected frequency (%)
ALIX ALIX	119	36.96	25
alix-2 ALIX	203	63.04	50
alix-2 alix-2	0	0	25

Supplemental Table 3. Segregation data from selfed *alix*-3 *ALIX* progeny.

Genotype	Observed	Observed frequency (%)	Expected frequency (%)
ALIX ALIX	143	35.4	25
alix-3 ALIX	261	64.6	50
alix-3 alix-3	0	0	25

Supplemental Table 4. Germination analysis of the progeny of *alix-2 ALIX* and *alix-3 ALIX* heterozygous plants compared to wild-type (*ALIX ALIX*) plants.

	Germinated	Not germinated	Total
ALIX ALIX	432 / 98,18%	8 / 1,82%	440
alix-2 ALIX	1005 / 85,03%	177 / 14,97%	1182
alix-3 ALIX	963 / 92,5%	78 / 7,5%	1041

Number of seedlings and percentages of the total are shown.

Supplemental Table 5. Transmission efficiency (TE) of the *alix-2* and *alix-3* alleles through male and female gametes.

Parental cross (Female x Male)	Nº of seedlings genotyped	*alix* alleles observed	*alix* alleles expected	TE (%)	P (χ^2 test)
WT x *alix-2 ALIX*	187	99	93.5	105.88	n.s
alix-2 ALIX x WT	100	27	50	54	<0.05
WT x *alix-3 ALIX*	46	23	23	100	n.s.
alix-3 ALIX x WT	54	30	27	111.1	n.s.

Supplemental Table 6. Protein identification details obtained with the ABi 4800 MALDI TOF/TOF mass spectrometer (AB SCIEX) and the GPS explorer v4.9 (AB SCIEX) software package combined with search engine Mascot version 2.5.10 (Matrix Science).

Identified Protein			MSMS data										
TAP-ALIX BAND	Locus	Description	Peptide Number	Observed	Mr(expt)	Mr(calc)	Delta(Da)	ppm	Start	End	Miss	Ions	Peptide	Variable Modification
1	At1g15130	BRO-1 like domain containing protein	1	1028,5	1027,49	1027,54	-0,05	-45,07	571	579	0	---	R.QLENLGAQR.A	
			2	1082,45	1081,44	1081,47	-0,03	-24,3	473	481	0	---	K.EATEDSQFR.S	
			3	1279,54	1278,53	1278,59	-0,06	-42,57	29	38	0	---	R.NYVTFTYSER.E	
			4	1279,54	1278,53	1278,59	-0,06	-42,57	29	38	0	47	R.NYVTFTYSER.E	
			5	1304,56	1303,55	1303,6	-0,05	-37,36	255	265	0	---	K.AALFYGEACFR.Y	
			6	1304,56	1303,55	1303,6	-0,05	-37,36	255	265	0	10	K.AALFYGEACFR.Y	
			7	1321,54	1320,53	1320,59	-0,06	-43,67	721	731	0	---	R.QMSGLSFQDHR.S	Oxidation (M)
			8	1595,64	1594,63	1594,7	-0,07	-45,15	599	611	0	---	K.LMTITGSYEDMFR.K	2 Oxidation (M)
			9	1695,78	1694,78	1694,85	-0,07	-41,91	269	282	1	---	K.ELHEKEEIAEEIAR.L	
			10	2089	2087,99	2088,08	-0,09	-40,66	122	141	0	---	K.AAVLFNLGASYSQIGLGHDR.T	
			11	2089	2087,99	2088,08	-0,09	-40,66	122	141	0	5	K.AAVLFNLGASYSQIGLGHDR.T	
			12	2291,95	2290,94	2291,04	-0,1	-45,6	713	731	1	---	R.DMIEDVQRQMSGLSFQDHR.S	
			13	2291,95	2290,94	2291,04	-0,1	-45,6	713	731	1	---	R.DMIEDVQRQMSGLSFQDHR.S	
			14	2323,93	2322,93	2323,03	-0,1	-45,85	713	731	1	---	R.DMIEDVQRQMSGLSFQDHR.S	2 Oxidation (M)
			15	2431,08	2430,07	2430,17	-0,1	-40,86	299	321	0	---	R.GAPAQLIEAMNTLESSIDGNLDR.A	Oxidation (M)
ALIX BAND	Locus		Peptide Number	Observed	Mr(expt)	Mr(calc)	Delta(Da)	ppm	Start	End	Miss	Ions	Peptide	Variable Modification
1	At1g15130	BRO-1 like domain containing protein	1	1082,43	1081,42	1081,47	-0,05	-41,13	443	451	0	---	K.EATEDSQFR.S	
			2	1304,55	1303,54	1303,6	-0,06	-48,95	225	235	0	---	K.AALFYGEACFR.Y	
			3	1304,55	1303,54	1303,6	-0,06	-48,95	225	235	0	15	K.AALFYGEACFR.Y	
			4	1695,77	1694,76	1694,85	-0,09	-48,76	239	252	1	---	K.ELHEKEEIAEEIAR.L	
			5	1772,78	1771,77	1771,86	-0,09	-48,03	149	165	0	---	R.QASHAFMAAAGAFAHLR.D	Oxidation (M)
			6	2088,98	2087,97	2088,08	-0,11	-48,18	122	141	0	---	K.AAVLFNLGASYSQIGLGHDR.T	
			7	2088,98	2087,97	2088,08	-0,11	-48,18	122	141	0	49	K.AAVLFNLGASYSQIGLGHDR.T	
			8	3349,52	3348,51	3348,67	-0,16	-46,19	304	334	1	---	R.VPSPSSLSPLPAFSMVKPMNMTDILDASKEK.M	2 Oxidation (M)

Peptide Number: Peptide index number within the list of peptides associated with a given protein. Observed: The observed monoisotopic mass of the peptide in the spectrum (m/z). Mr (Expt): The experimental mass of the peptide calculated from the observed m/z value. Mr (Calc): The theoretical mass of the peptide based on its sequence. Delta (Da): The difference between the theoretical (Mr (Calc)) and experimental (Mr (Exp)) masses, in daltons. ppm: RMS error of the set of matched mass values, in ppm. Start: The starting position of the peptide in the protein. End: The ending position of the peptide in the protein. Miss: Number of missed Trypsin cleavage sites. Peptide: The amino acid sequence of the selected peptide. Variable Modification: Variable modification type on the peptide.

Supplemental Table 7. Reporter lines used in this study as described in (Dettmer et al., 2006; Geldner et al., 2009).

Line	Localization	Tagged protein	Reference
WAVE 2	MVB	RabF2b	Geldner et al., 2009
WAVE 9	Vacuole	VAMP711	Geldner et al., 2009
WAVE 22	Golgi	SYP32	Geldner et al., 2009
WAVE 34	Recycling endosome	RabA1e	Geldner et al., 2009
VHA1-RFP	Early endosome	VHA1	Dettmer et al., 2006

Dettmer, J., Hong-Hermesdorf, A., Stierhof, Y.D., Schumacher, K., and Hong-Hermesdorf, A. (2006). Vacuolar H+-ATPase activity is required for endocytic and secretory trafficking in *Arabidopsis*. Plant Cell. 18:715–730.

Geldner, N., Denervaud-Tendon, V., Hyman, D.L., Mayer, U., Stierhof, Y.D., and Chory, J. (2009). Rapid, combinatorial analysis of membrane compartments in intact plants with a multicolor marker set. Plant J. 59, 169-178.

Supplemental Table 8. Analysis of intracellular Pi pools in roots of wild-type (WT) and *alix-1 PHR1* plants grown in Pi-sufficient media (500 mM).

Genotype	Glucose-6-P + Chloroplastic Pi	Cytosolic Pi	Vacuolar Pi
WT	2.62[a]	0.25	12.1
alix-1 PHR1	3.2	0.4	8.4
Increase or Reduction compared to WT levels (%)	18.27	37.25	-30.55

[a]Values correspond to areas under the corresponding peaks in ^{31}P-NMR experiments (see Figure 9).

Supplemental Table 9. Primers and probes (Roche) used in RT-qPCR analyses.

Locus	Gene	Probe N°	Primer sequence
At3g17790	*ACP5*	125	5: CCAAACTTCGAACAATCTTTCTC 3: GTTTCCCAAAACACTGTACCACT
At1g49240	*ACTIN8*	7	5: GACTCAGATCATGTTTGAGACCTTT 3: CCAGAGTCCAACACAATACCG
At1g15130	*AtALIX*	124	5: GTATCGAGAGATCAAGGAGAACATC 3: TTCACATTCGTGATTGCATCT
At3g52190	*PHF1*	55	5: TTTTGACCCCATTACTGCTTC 3: TCCTTAAGCGTGTGTGTTGC
At1g17710	*PMH1*	55	5: TCAACGAAATTATGTCATCAGAGG 3: TTTCAGAGCTCAACATCTTGTCA
At4g14090	*PRE8*	12	5: CGTGGAGGATTGGAGTGAA 3: TCTAATCTCCTCCCCATCCA
At4g33030	*SQD1*	22	5: CATCCTCTAAACCAAAGCGTGT 3: AGTAGCCCAACCGCAATAAC
At2g43920	*TMT1*	151	5: TGGAAACATTCTTCCTACTCCTG 3: CCGCCTTCTGCAACAACT